

# Static and dynamic properties of star-shaped honeycomb sandwich panels

Zhifei Yang<sup>a</sup>, Bojun Mao<sup>b</sup>

School of Sciences, Chang'an University, Shaanxi, China.

<sup>a</sup>[yzfdhr@163.com](mailto:yzfdhr@163.com); <sup>b</sup>2259955358@qq.com

**Abstract.** The star-shaped concave structure material is a new type of negative Poisson's ratio material, which combines the advantages of negative Poisson's ratio material and honeycomb material. The negative Poisson's ratio structure has very good mechanical properties, such as bearing capacity, impact resistance, and shear resistance. The honeycomb sandwich panel is a typical lightweight material with high specific strength, specific stiffness, and good energy absorption characteristics. In this paper, the star-shaped concave structure is used as the core layer of the sandwich panel, and the advantages of both the honeycomb sandwich panel and negative Poisson's ratio structure are combined to make a star-shaped honeycomb sandwich panel. In order to analyze the properties of this material, we use the finite element numerical simulation method to study the effects of several geometric parameters (element thickness, beam width, beam length, and star angle) on the bending stiffness, buckling critical load and natural frequency of honeycomb sandwich panels, which provides a new reference for the design optimization of star-shaped concave honeycomb sandwich panels in practical engineering applications.

**Keywords:** star-shaped concave honeycomb sandwich panel; negative Poisson's ratio; static and dynamic performance; buckling analysis; free vibration.

## 1. Introduction

Sandwich panel structure is considered an ideal material for explosion-proof and impact resistance, mainly because this material has excellent properties such as lightweight and efficient energy absorption. The different components of the sandwich panel structure can play different functions. When subjected to impact loads, the sandwich panel bears bending, compression, and tensile loads, while the core layer bears shear loads. Among them, the core structure plays a dominant role, and the space for improving the performance of the core is large. Common categories include honeycomb corrugated plates and so on. Reasonably designing the geometric configuration of honeycomb cells and matching them with appropriate materials can simultaneously obtain unique physical properties such as a negative Poisson's ratio. In recent years, with the development of industrial technology, porous honeycomb materials have been widely used for damage protection and how to improve their service performance has always been a hot topic in this field.

Among the numerous core forms, porous honeycomb structures have become the focus of researchers' attention due to their lightweight and designable characteristics. The cell shapes of porous honeycomb microstructures are generally rectangular, hexagonal, and so on. Compared to traditional dense materials, porous honeycomb materials have advantages such as low relative density, high specific stiffness, and strength, which satisfy the needs of engineering practice.

Most of the earliest honeycomb structures studied and analyzed are positive Poisson's ratio, but with the development of negative Poisson's ratio structure, honeycomb structures with negative Poisson's ratio performance have been continuously studied and found. Negative Poisson's ratio honeycomb has attracted wide attention because of its unique energy absorption ability and compression torsion. After the deformation of negative Poisson's ratio sandwich structure, its elements are always perpendicular to the curved surface, so that the strength and stiffness of materials can be used efficiently. It is found that under the same initial density, the negative Poisson's ratio material has higher yield strength and lower stiffness than the traditional material. Most of the earliest honeycomb structures studied and analyzed are positive Poisson's ratio, but with the development of

negative Poisson’s ratio structures, honeycomb structures with negative Poisson’s ratio performance have also been continuously examined. Negative Poisson’s ratio honeycomb has attracted widespread attention due to its unique energy absorption ability and compression torsion. After the deformation of the negative Poisson’s ratio sandwich structure, its elements are always perpendicular to the curved surface, enabling efficient utilization of the strength and stiffness performance of the material. Previous research has found that under the same initial density conditions, materials with negative Poisson’s ratio have higher yield strength and lower stiffness compared to traditional materials.

In summary, although a large number of research has been conducted on the load response and design issues of sandwich panel structures, there is still a gap in the optimization design of star concave honeycomb sandwich panels. It is a new direction worthy of in-depth exploration to analyze this sandwich panel with a new negative Poisson’s ratio honeycomb topology structure.

## 2. Research Contents

The research object of this paper is a sandwich panel composed of a regular array of star-shaped cells. A single cell is composed of one core layer (as shown in Figure 1b) and two panels. In the finite element model, the material of the star-shaped cells is iron, with a density of  $7.8 \text{ g} \cdot \text{cm}^{-3}$  and an elastic modulus of  $210 \text{ Pa}$ . The material of the panel is aluminum, with a density of  $2.7 \text{ g} \cdot \text{cm}^{-3}$  and an elastic modulus of  $70 \text{ Pa}$ . This study mainly changes the four geometric parameters shown in Figure b, namely  $t$ ,  $L1$ ,  $L2$ ,  $H$ , with a single cell size of  $50\text{mm} \times 50\text{mm} \times 10\text{mm}$ . For the convenience of modeling and analysis, we convert the magnitude of the star angle into the distance between the sharp corner of the star angle and the center of the cell, which is the length  $L2$ . The overall height of the cell is  $10\text{mm}$ , which is composed of the thickness  $h$  of the panel and the thickness  $H$  of the star-shaped inner core ( $2h+H=10\text{mm}$ ). Before conducting numerical simulations, this study conducts a convergence analysis of the grid to ensure the rationality of the three-point bending analysis, buckling analysis, and free vibration analysis.

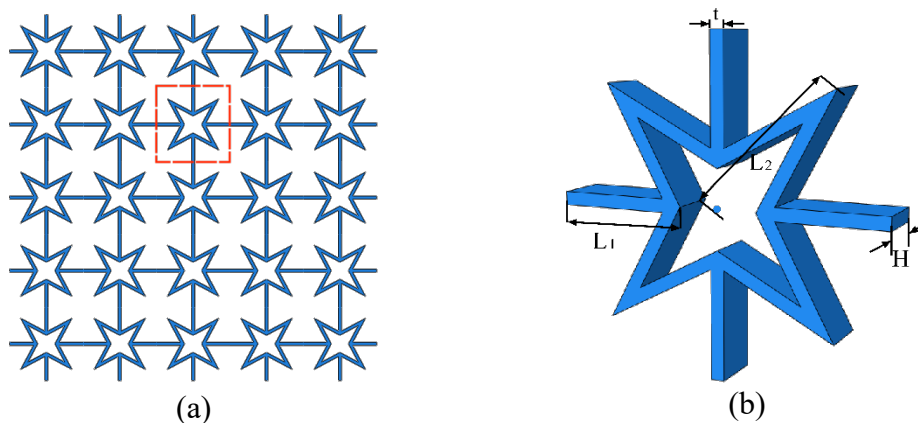


Fig. 1 Star-shaped Honeycomb Sandwich Panel and Its Cell Structure

Table 1 Parameter Design of Cell Geometry Size

	H (mm)	t (mm)	L1 (mm)	L2 (mm)
H-1	9.6	2.0	18	$15\sqrt{2}$
H-2	9.2	2.0	18	$15\sqrt{2}$
H-3	8.8	2.0	18	$15\sqrt{2}$
H-4	8.4	2.0	18	$15\sqrt{2}$
H-5	8.0	2.0	18	$15\sqrt{2}$
t-1	8.8	0.5	18	$15\sqrt{2}$
t-2	8.8	1.0	18	$15\sqrt{2}$

t-3	8.8	1.5	18	$15\sqrt{2}$
t-4	8.8	2.0	18	$15\sqrt{2}$
t-5	8.8	2.5	18	$15\sqrt{2}$
L1-1	8.8	2.0	10	$20\sqrt{2}$
L1-2	8.8	2.0	12	$20\sqrt{2}$
L1-3	8.8	2.0	14	$20\sqrt{2}$
L1-4	8.8	2.0	16	$20\sqrt{2}$
L1-5	8.8	2.0	18	$20\sqrt{2}$
L2-1	8.8	2.0	18	$10\sqrt{2}$
L2-2	8.8	2.0	18	$12.5\sqrt{2}$
L2-3	8.8	2.0	18	$15\sqrt{2}$
L2-4	8.8	2.0	18	$17.5\sqrt{2}$
L2-5	8.8	2.0	18	$20\sqrt{2}$

### 2.1 Three-point Bending Analysis

The finite element model of the three-point bending test is shown in Figure 2, and the supporting points at the left and right ends are 50 mm away from the edge of the honeycomb sandwich panel. The model applies a load on the sandwich panel by controlling the cylinder located above, causing it to move downward and squeeze the sandwich panel, and thus obtains the force-displacement curve of the honeycomb sandwich panel. In the three-point bending analysis model, we design the macroscopic size of the honeycomb sandwich panel to be 1000mm \* 500mm \* 10mm, which is composed of 50 \* 10 cell arrays. We adopt a C3D10 grid with the number of 66607 grids and 115941 nodes.

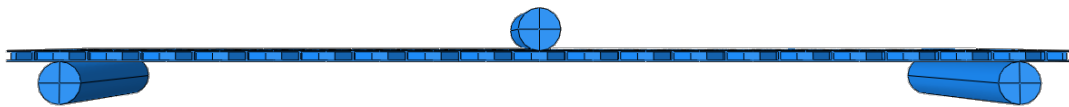


Fig. 2 Three-point Bending Model Diagram

### 2.2 Buckling Analysis

The finite element model of buckling analysis is shown in Figure 3. In the buckling analysis, three sides of the star-shaped honeycomb sandwich panel are constrained by completely fixed constraints, the remaining free sides are uniformly distributed, and the first six critical buckling loads and deformation diagrams corresponding to sandwich panels with different geometric parameters are obtained. In the finite element model of buckling analysis, the grid type is C3D10, the number of grids is 61915 and the number of nodes is 109293.

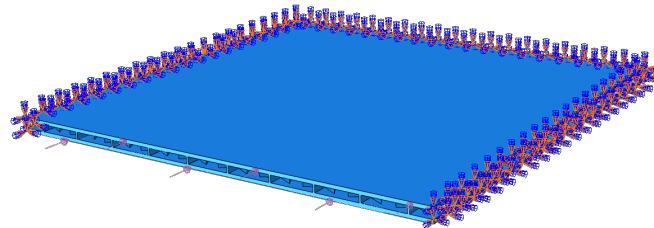


Fig. 3 Buckling Analysis Model Diagram

### 2.3 Free Vibration Analysis

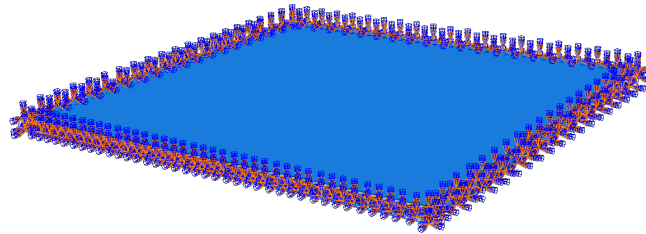


Fig. 4 Free Vibration Analysis Model diagram

In the free vibration analysis of the star-shaped honeycomb sandwich panel, the periphery of the sandwich panel is completely constrained, the first 8 natural frequencies of the model are calculated, and a deformation nephogram is drawn. In this model, we choose a C3D10 type grid with a total number of 61915 elements and 109293 nodes.

## 3. Result Analysis

### 3.1 Three-point Bending Analysis

In order to explore the influence of the thickness of star-shaped cells on the bending performance of sandwich panels, five groups of controlled variable tests are carried out by using the variable design scheme shown in Table 1, and the group numbers are H-1, H-2, H-3, H-4, H-4, and H-5 respectively. Through calculation, it can be found that the bending stiffness of sandwich panels increases with the increase of panel thickness because the bending moment provided by two panels accounts for the majority.

In order to further compare the economy of different sandwich panels, we adopt a new indicator: the ratio of bending stiffness to equivalent density  $k / \rho^*$ , where  $k$  is the slope of the force-displacement curve,  $\rho^*$  is the equivalent density of the star-shaped honeycomb sandwich panel. After calculation, we found that the ratio increases with the thickness of the panel, and the growth rate slows down as the thickness increases. Therefore, in practical engineering, it can be considered to appropriately increase the panel thickness, reduce material costs, and improve economic benefits while satisfying the performance requirements of engineering materials.

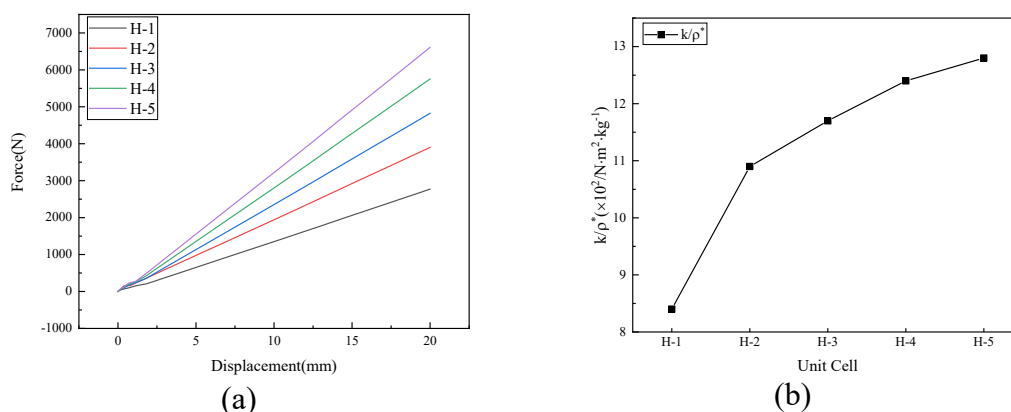


Fig. 5 Three-point Bending Analysis under Different Cell Thicknesses

In order to explore the effect of straight beam width on the bending performance of sandwich panels in star-shaped cells, we design a variable scheme as shown in Table 1, and conduct five sets of experiments. After calculation, we found that as the width of the straight beam increases, the bending performance does not change significantly, but the number of its  $k / \rho^*$  significantly decreases, that is, an increase in the width of the straight beam does not significantly enhance the bending performance, but significantly increases the material cost. Therefore, in engineering design,

the width of the straight beam in the star-shaped cell should be reduced to improve the efficiency while meeting the mechanical performance requirements.

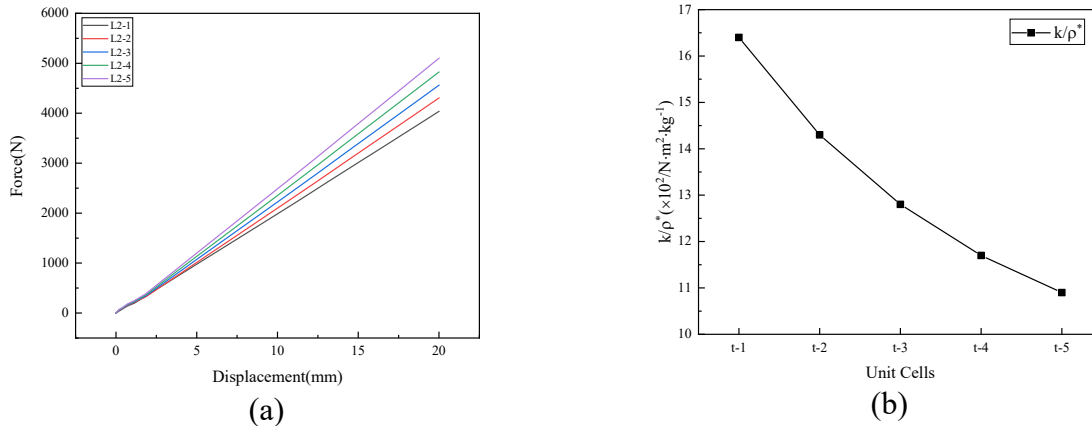


Fig. 6 Three-point Bending Analysis under Different Beam Width

In order to investigate the effect of straight beam length L1 on the performance of sandwich panels, we design control variable experiments with group numbers L1-1, L1-2, L1-3 and L1-4. L1-5, respectively. From the calculation results, it can be seen that as the length of the straight beam decreases, the bending performance of the panel does not significantly decrease, but the number of its  $k/\rho^*$  significantly increases. Therefore, in engineering design, the straight beam length L1 should be appropriately reduced to improve economic efficiency while satisfying the mechanical performance requirements.

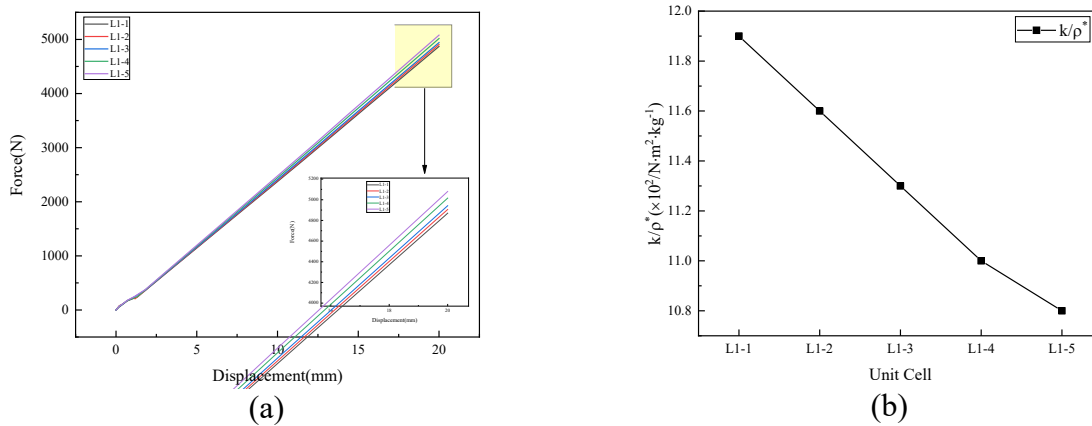


Fig. 7 Three-point Bending Analysis under Different Straight Beam Lengths

In order to investigate the influence of changes in star angle telescopic length L2 on the performance of sandwich panels, we design experiments with group numbers L2-1, L2-2, L2-3, L2-4, and L2-5, respectively. After calculation, we can see that as the star angle telescopic length decreases, the bending performance does not change significantly, but the number of its  $k/\rho^*$  significantly increases. Therefore, in engineering design, when meeting performance requirements, it is possible to appropriately reduce the star angle telescopic length to save materials and improve the economy.

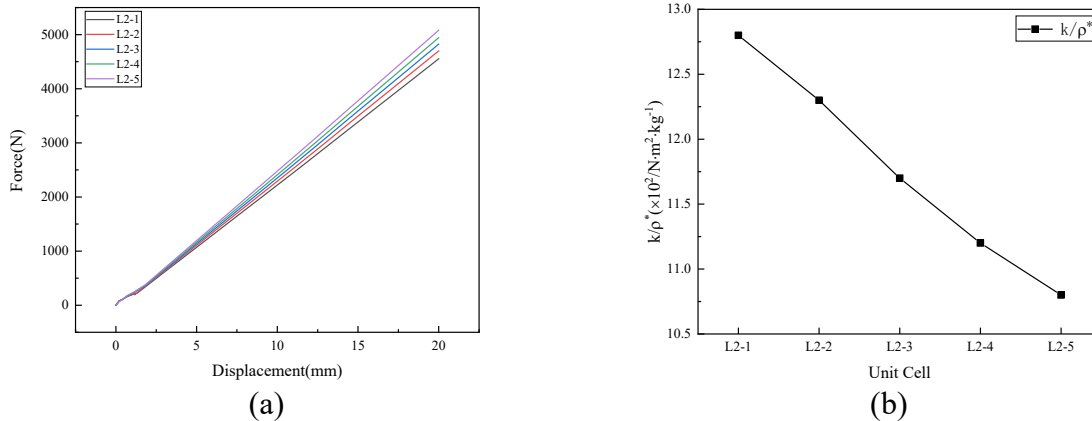


Fig. 8 Three-point Bending Analysis under Different Telescopic Lengths of Star Angles

### 3.2 Buckling Analysis

In order to investigate how the height of star-shaped cells affects the buckling state of star-shaped honeycomb sandwich panels, we adopt geometric models as shown in Table 1, and the group numbers are H-1, H-2, H-3, H-4, H-4, and H-5, respectively. After calculation, we found that as the height of the star-shaped cell decreases, the critical buckling load of the panel shows an increasing trend, mainly because the equivalent bending elastic modulus of the sandwich panel also increases. This change is understandable. When the star-shaped honeycomb sandwich panel is subjected to bending loads, the part above the neutral axis bears compressive stress, and the part below the neutral axis bears tensile stress. As we discussed earlier, the thicker the two panels, the greater the bending stiffness of the panel.

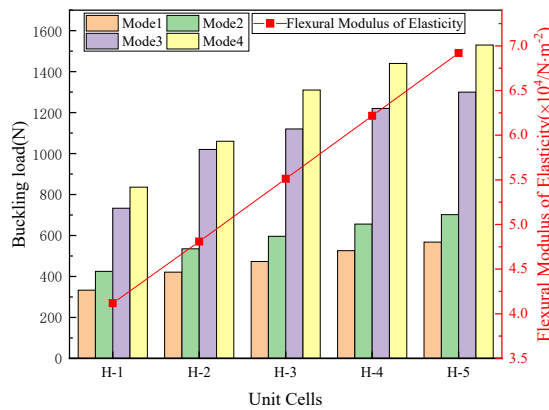


Fig. 9 Buckling Analysis under Different Cell Thicknesses

In order to investigate how the width  $t$  of the straight beam of the star honeycomb sandwich panel affects its buckling state, we used the variable design scheme shown in Table 1 for buckling modal analysis. From the calculation, it can be seen that as the width of the straight beam increases, the critical buckling load of the panel shows an increasing trend, mainly because the equivalent bending elastic modulus of the sandwich panel also increases, which is easy to understand. From the content we discussed earlier, as the width of the straight beam of the star-shaped honeycomb sandwich panel increases, its tensile and bending performance increases, but the growth rate is very small.

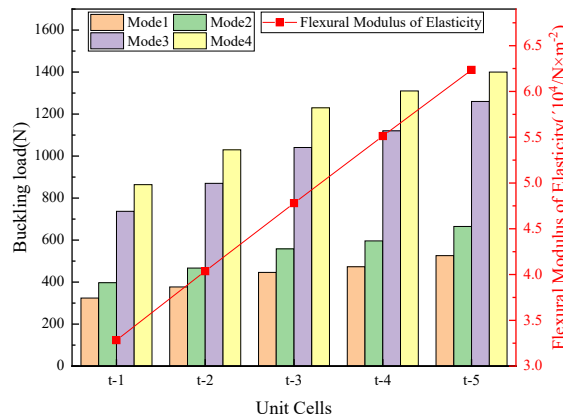


Fig. 10 Buckling Analysis of Straight Beams with Different Widths

In order to explore how the straight beam length L1 of the star-shaped honeycomb sandwich panel affects its buckling state, we use the model shown in Table 1 for buckling modal analysis. The calculation shows that with the increase of L1, the buckling critical load of sandwich panels first increases and then decreases. It reaches the maximum when the length is 16mm and decreases to the minimum when it is 18 mm. When L1 is 16mm, the planar load resistance in the panel is the strongest. When the length of L1 is small, the equivalent bending elastic modulus increases with the increase of L1. When the length of L1 is too long, the influence of equivalent bending elastic modulus on buckling critical load weakens. Obviously, the change in L1 length has little influence on the buckling critical load, which is easy to understand, because the influence of straight beam length on the equivalent bending elastic modulus of star-shaped honeycomb sandwich panel is limited.

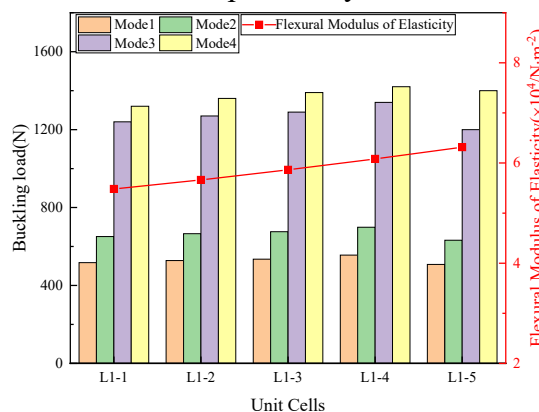


Fig. 11 Buckling Analysis of Straight Beams with Different Lengths

In order to investigate the effect of different star angle telescopic lengths on the buckling state, we conduct control variable experiments on group numbers L2-1, L2-2, L2-3, L2-4, and L2-5, respectively. According to the calculation, the critical buckling load of the panel decreases to the minimum when L2 is  $10\sqrt{2}$ mm and increases to the maximum when L2 is  $17.5\sqrt{2}$ mm. When L2 is  $10\sqrt{2}$ mm, the planar load resistance inside the panel is the smallest. The equivalent bending elastic modulus increases with the increase of L2, and the first-order buckling mode of the star honeycomb sandwich panel is not significantly influenced by the size of the star angle.



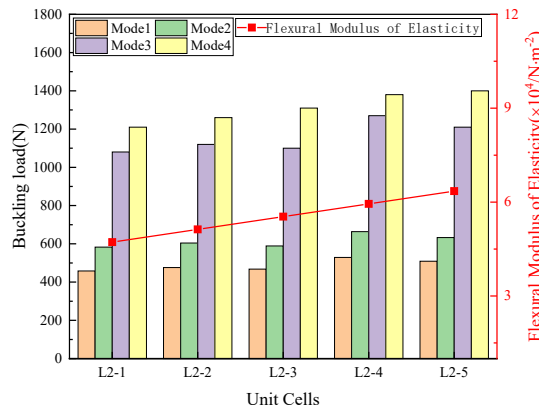


Fig. 12 Buckling Analysis under Different Telescopic Lengths of Star Angles

The difference in the buckling modal diagrams of the panels is not significant. Figure 13 shows the four-order modal diagram under the buckling test. From the figure, it can be seen that the first and second orders have a waveform in the x-axis direction and half a wave in the y-axis direction. The third order has two waveforms in the x-axis direction, one in the positive direction, one in the negative direction, and half in the y-axis direction. The center of the fourth-order modal image is concave and there is a slight waveform at the edge. In this case, the longer L1 and L2, the more obvious the waveform at the edge. For most modes, the center of panel deformation is close to the side where the load is applied, with only some fourth-order modal deformation centers located near the center of the panel.

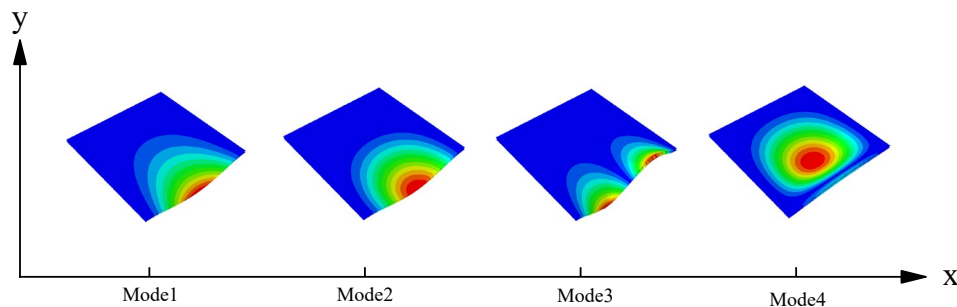


Fig. 13 Deformation Nephogram of Standard Panel in Buckling Analysis

### 3.3 Free Vibration Analysis

In order to investigate how the thickness of the star-shaped cell in the star-shaped honeycomb sandwich panel affects its free vibration state, we use the model shown in Table 1 for buckling modal analysis, and the group numbers are H-1, H-2, H-3, H-4, H-4, and H-5, respectively. As the thickness of the panel increases, the natural frequency of the star-shaped honeycomb sandwich panel increases, and the growth rate first increases and then slows down. As the thickness increases, the equivalent density of the panel also increases, and the growth rate remains basically unchanged. The variation of natural frequency is related to the stiffness and mass of the sandwich panel. In the previous bending and buckling analysis, we discussed that the equivalent stiffness of the five models H-1, H-2, H-3, H-4, H-4, and H-5 increases with the increase of panel thickness, which is related to the increasing trend of natural frequency. Figure 14(b) shows the variation of specific stiffness with thickness. It is evident that the H-1 model has a higher specific stiffness, and this geometric parameter model can be appropriately selected in engineering practice to improve economic benefits.



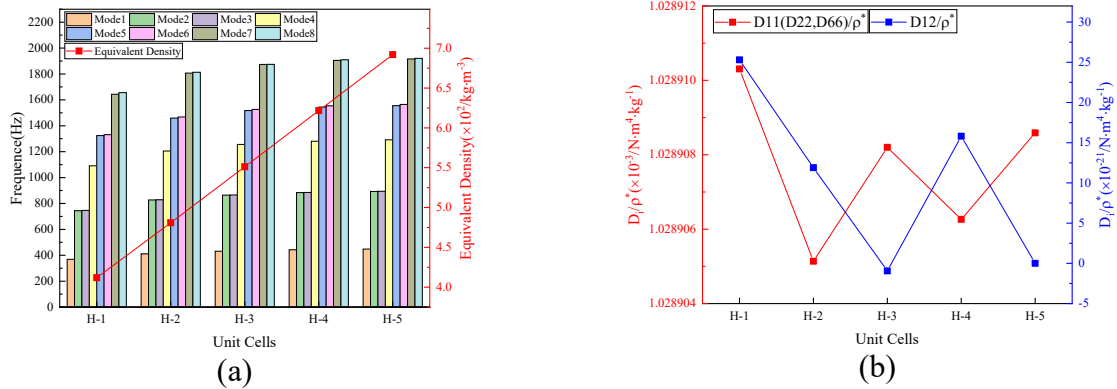


Fig. 14 Free Vibration Analysis under Different Cell Thicknesses

In order to investigate how the length of a straight beam affects the free vibration of a sandwich panel, we use the model shown in Table 1 for buckling modal analysis. From the calculation, it can be seen that as the length of L1 increases, the natural frequency of the sandwich panel first increases and then decreases, reaching its maximum at a straight beam length of 14mm and reaching its minimum at an L1 length of 18mm. As L1 increases, the equivalent density of the panel continues to increase, and the growth rate remains basically unchanged. This is understandable. As L1 increases, the cells occupy more space, and the equivalent density increases. The variation of natural frequency is related to the stiffness and mass of the sandwich panel. In the previous bending and buckling analyses, we discussed the trend of equivalent stiffness with increasing L1 length, which is related to the increasing trend of natural frequency. Figure (b) shows the variation of specific stiffness with L1 length. It is evident that the L1-2 model has a higher specific stiffness, and in engineering practice, this geometric parameter model can be appropriately selected to improve economic benefits.

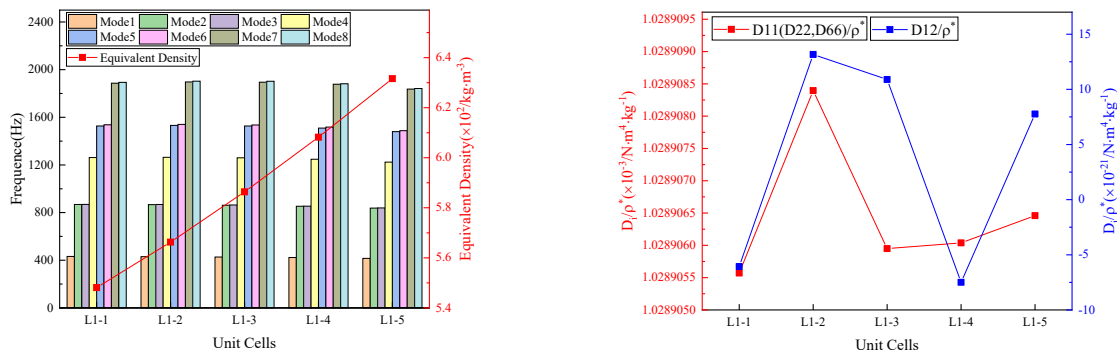


Fig. 15 Free Vibration Analysis under Different Straight Beam Widths

In order to investigate how the size of the star angle affects the free vibration state of the star-shaped cell in the star-shaped honeycomb sandwich panel, we use models with group numbers L2-1, L2-2, L2-3, L2-4, and L2-5 for analysis. As the telescopic length of the star angle increases, the natural frequency of the star-shaped honeycomb sandwich panel first increases and then decreases, reaching its maximum at a length of  $17.5\sqrt{2}$ mm in L2 and reaching its minimum at a length of  $20\sqrt{2}$ mm in L2. However, the overall variation is stable and the amplitude of change is small. As L2 increases, the equivalent density of the panel continues to increase, and the growth rate remains basically unchanged, which is easy to understand. Figure 16(b) shows the variation of specific stiffness with L2 length. It is evident that the L2-4 model has a higher specific stiffness, and this geometric parameter model can be appropriately selected in engineering practice to improve economic benefits.

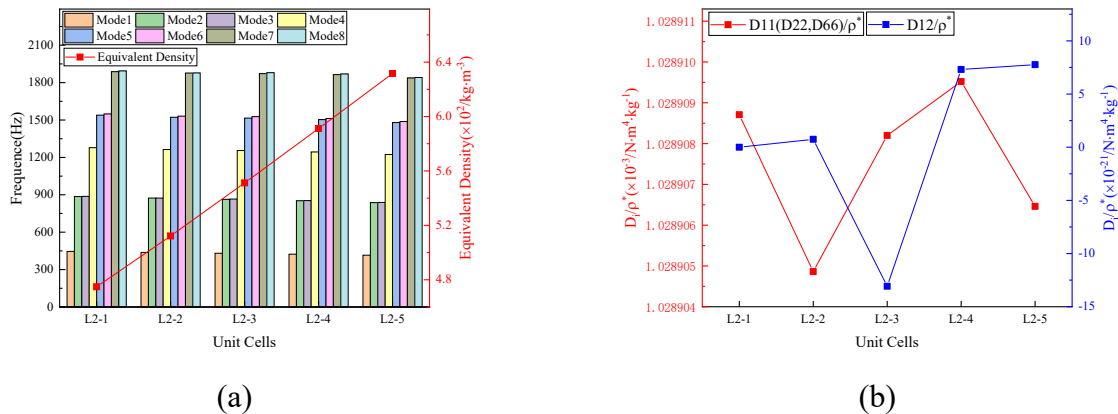


Fig. 16 Free Vibration Analysis of Telescopic Length of Different Star Angles

In order to investigate how the width of the straight beam in the star cell of the star-shaped honeycomb sandwich panel affects its free vibration state, we use the model shown in Table 1 for buckling mode analysis, with group numbers t-1, t-2, t-3, t-4, and t-5. As the width of the straight beam increases, the natural frequency fluctuation of the star-shaped honeycomb sandwich panel reaches its maximum at a straight beam width of 0.5mm and its minimum at a straight beam width of 2mm. As the width of the straight beam increases, the equivalent density of the panel continues to increase, and the growth rate remains basically unchanged. The variation of natural frequency is related to the stiffness and mass of the sandwich panel. Figure 17(b) shows the variation of specific stiffness with the width of the straight beam. It is evident that the specific stiffness is greatly affected by the width of the straight beam. In engineering practice, this geometric parameter model can be appropriately selected to improve economic benefits.

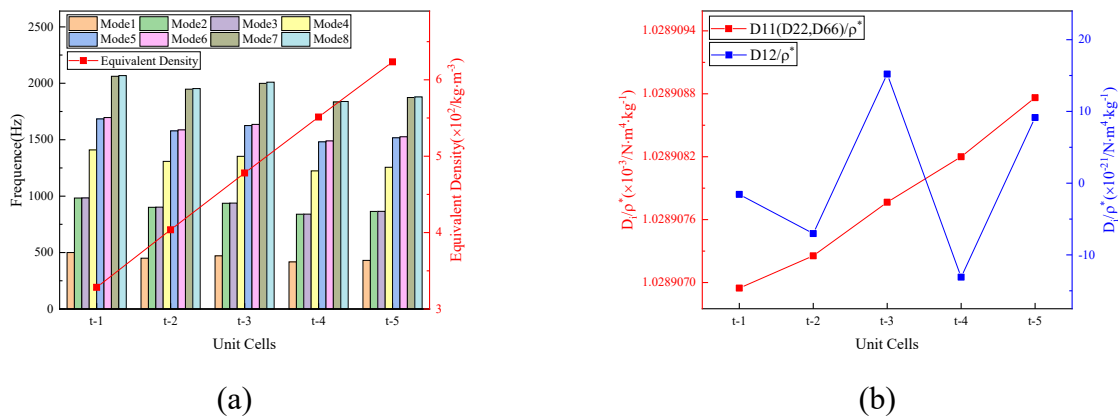


Fig. 17 Free Vibration Analysis of Different Straight Beam Widths

The vibration mode nephogram of the star-shaped honeycomb sandwich panel is shown below, and their common feature is that the deformation is located near the center of the panel. The first mode has only one wave in both the x-axis and y-axis directions, while the second and third modes are rotationally symmetric, with two waves in both the x-axis and y-axis directions. The four deformation regions in the fourth mode are located on the four diagonals of the square plate. The four deformation regions of the fifth mode are symmetrically distributed on two central axes. There is significant deformation in the center of the sixth mode shape, with narrow deformation areas along the edges. The deformation of the seventh and eighth vibration modes exhibits rotational symmetry, with protrusions at both ends and a narrow and low deformation area in the middle.

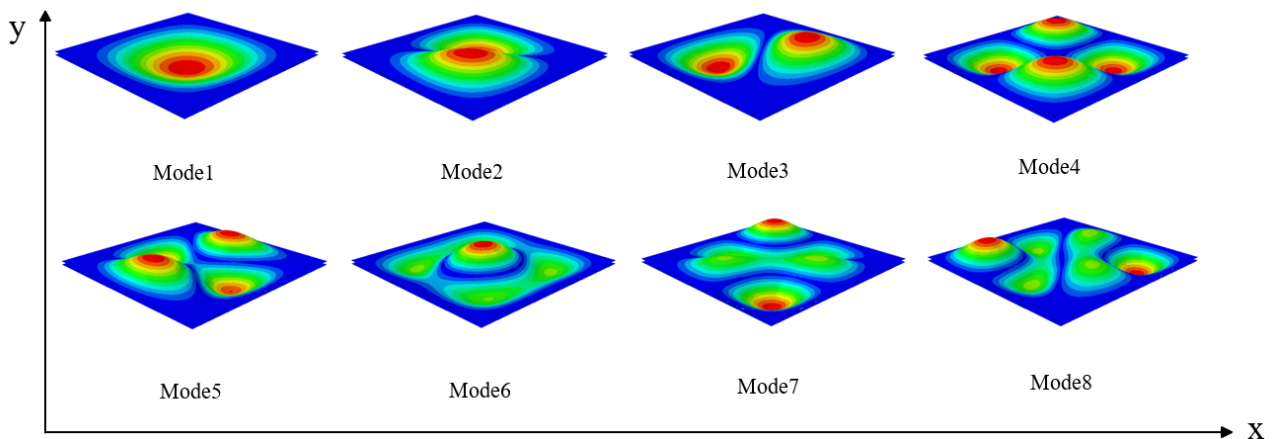


Fig. 18 Deformation Nephogram of Standard Panel in Free Vibration Analysis

#### 4. Conclusion

In this paper, the static and dynamic performance of star-shaped concave honeycomb sandwich panels is analyzed. The core of the sandwich panel is a concave star-shaped structure with a negative Poisson's ratio, and there is a lack of research on the static and dynamic performance system of this structure in related fields. In this paper, the influence of different geometric parameters on the bending performance, buckling performance, and vibration characteristics of sandwich panels is analyzed, which lays a foundation for further research and practical engineering application of star-shaped honeycomb sandwich panels.

(1) Summarizing the influence of different parameters on the static and dynamic performance of star-shaped honeycomb sandwich panels. The bending stiffness of the sandwich panel increases with the increase in panel thickness. With the increase of straight beam width, the bending performance of the sandwich panel does not change significantly. With the increase of straight beam length, the bending performance of the sandwich panel increases, but the increase is not significant. When the telescopic length of the star angle increases, the bending performance is enhanced, but the increase is limited. Considering the actual economic benefits of the project, the length of the straight beam and the star angle can be appropriately reduced to save the cost under the condition of meeting the requirements of mechanical properties.

(2) Further research may analyze the dynamic performance of the star-shaped concave honeycomb sandwich panel, and explore its response under ballistic impact and permanent compression under extreme load.

#### References

- [1] Ahmed, Sameh, and Khaled Galal. 2017. "Effectiveness of FRP Sandwich Panels for Blast Resistance." *Composite structures* 163(Journal Article): 454–64.
- [2] Argatov, Ivan I., Raúl Guinovart-Díaz, and Federico J. Sabina. 2012. "On Local Indentation and Impact Compliance of Isotropic Auxetic Materials from the Continuum Mechanics Viewpoint." *International journal of engineering science* 54(Journal Article): 42–57.
- [3] Arora, H., P. Del Linz, and J. P. Dear. 2017. "Damage and Deformation in Composite Sandwich Panels Exposed to Multiple and Single Explosive Blasts." *International journal of impact engineering* 104(Journal Article): 95–106.
- [4] Bai, Zhonghao et al. 2015. "Optimal Design of a Crashworthy Octagonal Thin-Walled Sandwich Tube under Oblique Loading." *International journal of crashworthiness* 20(4): 401–11.

- [5] Chen, C. P., and R. S. Lakes. 1991. "Holographic Study of Conventional and Negative Poisson's Ratio Metallic Foams - Elasticity, Yield and Micro-Deformation." *Journal of materials science* 26(20): 5397–5402.
- [6] Chen, Zihao et al. 2021. "Dynamic Response of Sandwich Beam with Star-Shaped Reentrant Honeycomb Core Subjected to Local Impulsive Loading." *Thin-Walled Structures* 161: 107420.
- [7] Cheng, Yuansheng et al. 2018. "The Effects of Foam Filling on the Dynamic Response of Metallic Corrugated Core Sandwich Panel under Air Blast Loading – Experimental Investigations." *International journal of mechanical sciences* 145(Journal Article): 378–88.
- [8] Choi, J. B., and R. S. Lakes. 1992. "Non-Linear Properties of Metallic Cellular Materials with a Negative Poisson's Ratio." *Journal of materials science* 27(19): 5375–81.
- [9] CHOI, J. B., and R. S. LAKES. 1996. "Fracture Toughness of Re-Entrant Foam Materials with a Negative Poisson's Ratio : Experiment and Analysis." *International journal of fracture* 80(1): 73–83.
- [10] Chunpeng, LI, ZHANG Pan, LIU Jun, and CHENG Yuansheng. 2018. "Numerical Simulation of Dynamic Response of Functionally Graded Aluminum Foam Sandwich Panels under Air Blast Loading." *Zhongguo Jianchuan Yanjiu* 13(3): 77–84.
- [11] Dey, Chitralkha, and Sunil Nimje. 2016. "Experimental and Numerical Study on Response of Sandwich Plate Subjected to Blast Load." *Experimental techniques (Westport, Conn.)* 40(1): 401–11.
- [12] Dong, Jinyu et al. 2021. "Dynamic Response Characteristics and Instability Criteria of a Slope with a Middle Locked Segment." *Soil dynamics and earthquake engineering (1984)* 150(Journal Article): 106899.
- [13] Ebrahimi, Hamid, Leila Keyvani Someh, Julian Norato, and Ashkan Vaziri. 2018. "Blast-Resilience of Honeycomb Sandwich Panels." *International journal of mechanical sciences* 144(Journal Article): 1–9.
- [14] Feng, Li-Jia, Guang-Tao Wei, Guo-Cai Yu, and Lin-Zhi Wu. 2019. "Underwater Blast Behaviors of Enhanced Lattice Truss Sandwich Panels." *International journal of mechanical sciences* 150(Journal Article): 238–46.
- [15] Hundley, Jacob M., Eric C. Clough, and Alan J. Jacobsen. 2015. "The Low Velocity Impact Response of Sandwich Panels with Lattice Core Reinforcement." *International journal of impact engineering* 84(Journal Article): 64–77.